J. Phys. D: Appl. Phys. **42** (2009) 135205 (9pp) doi:10.1088/0022-3727/42/13/135205

Absolute transition probabilities for 559 strong lines of neutral cerium

J J Curry

National Institute of Standards and Technology, Gaithersburg, MD 20899-8422, USA

E-mail: jjcurry@nist.gov

Received 23 April 2009, in final form 20 May 2009
Published 17 June 2009
Online at stacks.iop.org/JPhysD/42/135205

Abstract
Absolute radiative transition probabilities are reported for 559 strong lines of neutral cerium covering the wavelength range 340–880 nm. These transition probabilities are obtained by scaling published relative line intensities (Meggers *et al* 1975 *Tables of Spectral Line Intensities (National Bureau of Standards Monograph 145)*) with a smaller set of published absolute transition probabilities (Bisson *et al* 1991 *J. Opt. Soc. Am.* B **8** 1545). All 559 new values are for lines for which transition probabilities have not previously been available. The estimated relative random uncertainty of the new data is ±35% for nearly all lines.

1. Introduction

The rare-earth element cerium has a particularly rich, even by rare-earth standards, optical emission spectrum from both its neutral and singly ionized stages. This characteristic has made cerium attractive for use in high-intensity discharge light sources where it improves both luminous efficacy and colour rendering.

Neutral cerium's complex spectrum has been a daunting challenge for both experimentalists and theorists, and there is still much work to be done on determination of atomic parameters. Of greatest significance among published work on neutral cerium is Martin's extensive energy level analysis [3–5], Meggers, Corliss, and Scribner's original [6] and revised [1] lists of nearly 1000 observed line intensities, and Bisson's *et al* [2, 7] measurement of 255 transition probabilities. Also of great significance is Martin's unpublished line list containing approximately 20 000 classified lines over the range 338.5–1000 nm. The size of this list gives a sense of the great extent of the problem of neutral cerium! Of lesser importance for this work are the observation of 1100 infrared lines by Verges *et al* [8], the measurement of 18 radiative lifetimes by Xu *et al* [9], and the measurement of two radiative lifetimes by Li *et al* [10].

In this work, we present absolute radiative transition probabilities for 559 strong spectral lines of neutral cerium. Transition probabilities have not been previously available for any of these lines. The new data are obtained by putting the relative line intensities of Meggers, Corliss and Scribner [1] on an absolute scale using the much smaller set of absolute transition probabilities obtained by Bisson *et al* [2].

The motivation for this effort is the determination of transition probabilities to enable simulation of the broad spectral distribution of emission from neutral cerium in high-intensity discharge light sources. The complexity of this and other rare-earth spectra necessitates the use of transition probabilities for several thousand lines, many more than are presented here. However, this work demonstrates a method that is better suited to obtaining sufficiently accurate values for such a large number of lines than is the more traditional method of combining lifetime measurements with branching fraction measurements [11]. The latter is generally capable of producing values with uncertainties in the range 5–10%, but requires considerably more effort and therefore more time. The estimated random (Type A) uncertainty of nearly all the values given here is ±35%[1]. For the purposes of simulating broad spectral distributions of very dense spectra, this level of uncertainty is more than sufficient. If the errors in individual values are truly random, those errors will begin to cancel rapidly in a low resolution spectrum as the density of lines increases. Thus the tradeoff of accuracy for efficiency is acceptable. We hope this method will provide the means for obtaining transition probabilities for most of the 20 000 classified lines of neutral cerium in future work.

2. The Bisson transition probabilities

Bisson *et al* [2] determined absolute transition probabilities for 30 transitions of neutral cerium by combining radiative lifetimes of several levels with the branching fraction for the

[1] All uncertainty values reported for this work are 1-σ values. Uncertainties quoted from other works are believed to be 1-σ values.

principal line originating from each of those levels. The lifetimes were measured with delayed laser photo-ionization. The branching fractions were determined from observations of emission from an electrodeless discharge lamp using a 1 m Fourier transform spectrometer. The stated uncertainty in the resulting transition probabilities is ±12%.

In addition, Bisson *et al* used their directly measured transition probabilities to construct a Boltzmann plot from which they extracted, under the assumption of a Boltzmann population of excited levels, a discharge temperature of 5000 ± 114 K. They then combined an additional 219 observed emission intensities with level populations determined from their Boltzmann plot to obtain absolute transition probabilities for those additional transitions. They corrected their observed intensities for self-absorption. They did not correct their intensities for line-of-sight effects. In other words, their intensities were integrated along the line of observation, which crossed through regions of differing temperatures.

Subsequently, Bisson *et al* [7] used time-resolved laser photo-ionization to directly measure transition probabilities for 6 transitions of neutral cerium, two of which overlapped and confirmed their earlier measurements [2]. A total of 253 transition probabilities were obtained by Bisson and coworkers. These are the only measured transition probabilities for neutral cerium of which we are aware[2].

3. The Meggers intensities

Meggers *et al* [1] published an extensive set of observed line emission intensities for the first and second spectra of 70 different elements, including neutral cerium. (We will refer to these as the Meggers intensities.) One of the primary goals of that work was to put spectrochemical analysis on a quantitative footing by providing a definite link between the relative intensities of various spectra observed in a standard source and the relative number of radiating atoms. Obviously, this also included putting the relative intensities within each spectrum, when observed in a standard source, on a quantitative scale. Prior to this effort, relative line intensities were a completely subjective matter and were useful only when comparing adjacent lines in a given spectrum.

The Meggers intensities were obtained from a 10 A direct current arc burning in air. The element of interest was introduced into the arc through electrodes formed from compressed copper powder and 0.1 at% of the element. According to Meggers, Corliss and Scribner, 'The arc was imaged on the collimator of a concave-grating spectrograph by means of a quartz lens immediately in front of the slit to obtain uniform illumination along its length and collect light from all parts of the arc.' Line intensities were recorded on photographic plates and a rotating step sector was used to simultaneously create several different exposure levels in order to calibrate the non-linear plate response. Copper line intensities provided an internal calibration for each observation, with the copper lines calibrated, in turn, on an absolute intensity scale by the use of a tungsten strip lamp for the wavelength range 330–900 nm. This range covers all of the transitions of neutral cerium appearing in the Meggers intensities.

The small quantities of the observed element released into the arc from the copper electrodes reduced the occurrence of self-absorption. Although self-absorption was later recognized to be a problem [12] for some lines of extraordinary intensity (much greater than 10 000 on the Meggers intensity scale of 1–90 000), none of the intensities in the neutral cerium spectrum is strong enough (all less than 400) to be influenced by this effect.

The Meggers intensities include values for 908 separate classified transitions in neutral cerium. The wavelengths and classifications for those lines were taken from the published [3] and unpublished work of Martin. By comparison of their results with several independent measurements of intensities and transition probabilities, Meggers, Corliss and Scribner estimated the general uncertainty in their relative intensities within a spectrum to be within the range of 15% and 25%.

4. The Martin line list

In his analysis of the spectrum of neutral cerium [3], Martin created an extensive list of observed lines that he was able to classify (assign to a transition between a specific pair of energy levels). This list contains measured wavelengths for approximately 20 000 lines in the range 338.5–999.9 nm, but has not been published because it is still considered by Martin to be preliminary.

Martin's unpublished line list is of interest here because one or more earlier versions of it were used by Corliss, in consultation with Martin, to develop the classifications in Meggers *et al* [1]. We have used the higher precision wavelength and energy level values of Martin in place of the lower precision values of Meggers, Corliss and Scribner.

5. Absolute transition probabilities from the Meggers intensities

Meggers, Corliss and Scribner believed that their intensity values might be used to derive absolute transition probabilities provided the source temperature was accurately known. In fact, Allen [13, 14] had already attempted something similar by the time the Meggers intensities were originally published [6]. The basis for that and many subsequent analyses is the relation between local emission intensity and absolute transition probability when the atoms in an optically thin emitting gas have a Boltzmann population distribution,

$$I(\vec{r}, \lambda_{\mathrm{ul}}) = \frac{hc}{4\pi\lambda_{\mathrm{ul}}} \frac{g_{\mathrm{u}}}{g_0} A_{\mathrm{ul}} N_0(\vec{r}) \exp^{-E_{\mathrm{u}}/kT(\vec{r})}. \qquad (1)$$

Here $I(\vec{r})$ is the emitted power per unit volume per unit solid angle at location $\vec{r}$ within the discharge, u and l refer to upper and lower levels, respectively, λ is the transition wavelength, A is the absolute transition probability, g is the level degeneracy, N_0 is the ground level population, E_u is the upper energy level

[2] J E Lawler and E A Den Hartog at the University of Wisconsin are currently analysing lifetime and branching fraction data for neutral cerium and are expected to produce absolute transition probabilities for a few thousand lines.

value, and h, c and k are fundamental constants with their usual definitions. Using the preceding relationship, their own intensities and independently measured absolute transition probabilities for a few spectra, Meggers, Corliss and Scribner derived a temperature for their arc of 5000 ± 300 K.

Early efforts to convert the Meggers intensities into absolute transition probabilities [15] using equation (1) produced highly inaccurate results, as shown, for example by Bridges and Wiese [16]. At least some of the inaccuracies are attributable to the adoption of the 'preliminary' equilibrium temperature given by Meggers, Corliss and Scribner to describe all lines.

The primary difficulty with a simple analysis based on equation (1) is that the Meggers intensity observations were not of a local emission intensity, but included contributions from all parts of their arc. This is true because Meggers, Corliss and Scribner did not image the arc on the entrance slit of their spectrograph but allowed the arc to uniformly illuminate it. Even if they had imaged the arc on the entrance slit, the observations would have consisted of an integral of local emission along the line of sight. The Meggers intensities, $I_M(\lambda_{ul})$, are an integral over the arc volume, V, and a solid angle of light collection, Ω, with an undetermined weighting factor, F,

$$I_M(\lambda_{ul}) = \int_\Omega d\Omega \int_V d^3\vec{r}\ F(\vec{r}, \Omega) \frac{hc}{4\pi\lambda_{ul}} \frac{g_u}{g_0} A_{ul} N_0(\vec{r}) \times \exp^{-E_u/kT(\vec{r})}. \quad (2)$$

Cowley [12] and, later, Cowley and Corliss [17] surmounted this difficulty by proceeding 'on a purely empirical basis without becoming involved in more fundamental questions such as the existence of a Boltzmann distribution of energy levels in the US National Bureau of Standards (NBS) copper arc, or whether the arc model should change significantly from one element to another.' They asked only whether the observed intensities could be described by equation (1) with some 'effective' temperature or temperatures, without regard to whether those temperatures had a physical interpretation.

They proceeded by making use of the best available A-values for some of the transitions observed by Meggers *et al* in several spectra. They allowed for the possibility of intensity-dependent and wavelength-dependent corrections to the observed intensities. They also allowed for the possibility of a non-Boltzmann population of excited states by including higher-order terms in the excitation energy. In only one case did they find a higher-order term useful. Likewise, no wavelength-dependent correction to the intensities was evident and only a small intensity-dependent correction was found useful.

Although Cowley [12] and Cowley and Corliss [17] showed that the relationship between the Meggers intensities and independently measured transition probabilities can be described by a modified form of equation (1), the 'effective' temperature turned out to be different for different spectra. Cowley and Corliss reported temperatures ranging from 5159 K for a subset of neutral cobalt lines to 8357 K for singly ionized neodymium [17]. They used their results and the Meggers intensities to obtain values for transitions for which no transition probability measurements were then available. They estimated the general uncertainty in these values to be $\pm 50\%$. The Bisson transition probabilities for neutral cerium did not exist at that time.

The temperature values derived in the above manner are without physical interpretation, but it is not surprising that different temperatures are obtained for different spectra. For example, spatial segregation of different elements and ionization stages is frequently observed in high current arcs. This includes a relative predominance of ion emission from the core of the arc. Furthermore, the presence of even relatively small amounts of some species can affect the arc temperature. Generally, Cowley's results indicated lower temperatures for neutral spectra than for singly ionized spectra, and lower temperatures for neutrals with lower ionization potentials.

6. Absolute transition probabilities for neutral cerium

Here we adopt an approach similar to that of Cowley [12]. (This approach was also used by Haverlag [18] for neutral cerium, although he reported no new transition probabilities.) That is, we use the relation

$$I_M(\lambda_{ul}) = \beta \frac{g_u A_{ul}}{\lambda_{ul}} \exp^{-E_u/kT} \quad (3)$$

to describe the Meggers intensities, with T and β being free parameters. The constant β consists of several factors including those related to light collection efficiency. Since the Meggers intensities are based on an arbitrary unitless scale, β has the units of nm s. The wavelength dependence of the collection efficiency has presumably been removed by experimental calibration. How well this reduced description of the arc relates the Meggers intensities to the Bisson absolute transition probabilities will be apparent when we determine values for T and β with lines common to both sets of data.

The Meggers list contains entries for 908 separate classified lines. We disregard 3 of these lines because they are described as blends. We also disregard an additional 19 lines because they are given multiple classifications. Of the remaining 886 lines, 11 have wavelength values that do not match any entry in the latest version of the Martin line list within 0.0015 nm. An additional 124 lines, although singly classified by Meggers, Corliss and Scribner, are multiply classified by Martin. Three more lines in the Meggers list have different classifications than those given by Martin. That leaves 748 lines for which the Meggers list and the Martin list agree with each other on wavelength and a single classification.

Of the 253 transitions for which Bisson *et al* [2] obtained transition probabilities and the 748 transitions from Meggers *et al* [1], 189 transitions are common to both sets. For these lines we calculated a least-squares linear fit to $\ln(I_M\lambda_{ul}/g_u A_{ul})$ versus E_u and obtained

$$T = 6590 \pm 220\,\mathrm{K}, \quad (4)$$

$$\beta = 0.037 \pm 0.006\,\mathrm{nm\,s}. \quad (5)$$

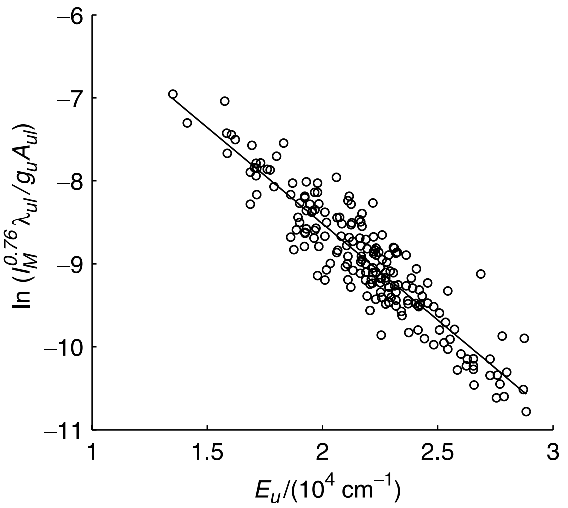

Figure 1. Boltzmann plot for 123 lines of neutral cerium, with the observed intensities, I_M, from Meggers *et al* [1] and the transition probabilities, g_uA_{ul}, from Bisson *et al* [2].

In making the fit, the data points were weighted according to the given uncertainties in the measured gA values (ranging from 12% to 19%) and estimated 25% average uncertainty in the Meggers intensities.

We explored the possibility that a correction to the intensity scale could improve the fit to the data points. We found that compressing the intensity scale, which ranged from 10 to 140, by the power 0.76 reduced the relative standard deviation in the fit from 0.32 to 0.30, yielding

$$T = 6200 \pm 200\,\mathrm{K}, \qquad (6)$$

$$\beta = 0.021 \pm 0.003\,\mathrm{nm\,s}. \qquad (7)$$

Our correction is compatible with Cowley and Corliss's [17] intensity-scale corrections ranging from $I^{0.63}$ to $I^{1.18}$ for eight different spectra. The Boltzmann plot using the intensity-scale correction is given in figure 1.

We also explored the possibility that the Meggers intensity scale drifted with wavelength. We did not find any significant effect, nor did Cowley and Corliss [12, 17].

Finally we explored the possibility that the data points are better represented by a non-linear curve on the Boltzmann plot by using a quadratic least-squares fit to the data. The quadratic term resulted in a small improvement in the relative standard deviation without the intensity scale adjustment, but was not required when the intensity-scale adjustment was used. Therefore, we did not use quadratic or higher-order terms. Cowley and Corliss [12, 17] generally did not find quadratic or higher-order terms useful either.

The Meggers list contains intensity values for an additional 559 transitions for which Bisson did not measure absolute transition probabilities. Absolute transition probabilities for those transitions can be obtained from the Meggers intensities using equation (3) and the derived values $T = 6200$ K and $\beta = 0.021$ nm s. These new gA values are given in table 1.

The Boltzmann parameters T and β are determined by lines whose upper levels lie in the range 13 514–28 850 cm^{-1}.

Table 1. g_uA_{ul} values derived from the Meggers intensities [1] for prominent lines of neutral cerium. Wavelengths, λ, are from Martin's unpublished line list. Energy level values, E, and J-values for both upper, u, and lower, l, levels are from Martin *et al* [3]. For gA values marked with an asterisk, the estimated uncertainty is ±50%. For all other gA values the estimated uncertainty is ±35%.

λ (nm)	E_u (cm^{-1})	J_u	E_l (cm^{-1})	J_l	g_uA_{ul} (s^{-1})
343.7816	29 079.931	4	0.000	4	2.1×10^{8}*
353.1623	30 686.340	3	2378.827	2	2.6×10^{8}*
362.8612	29 759.552	4	2208.657	5	3.2×10^{8}*
366.6013	27 269.831	3	0.000	4	1.8×10^{8}
366.6040	27 269.619	4	0.000	4	1.8×10^{8}
368.6044	29 330.295	4	2208.657	5	2.9×10^{8}*
373.1254	28 072.439	4	1279.424	4	1.2×10^{8}
373.2559	30 759.782	5	3976.104	6	3.0×10^{8}*
374.2211	26 943.447	2	228.849	2	9.8×10^{7}
374.2247	26 714.323	3	0.000	4	7.0×10^{7}
374.3972	26 702.035	5	0.000	4	1.7×10^{8}
379.3834	26 351.090	4	0.000	4	9.6×10^{7}
379.9092	27 594.029	5	1279.424	4	1.6×10^{8}
380.3832	26 510.686	1	228.849	2	6.7×10^{7}
387.3036	27 091.644	4	1279.424	4	2.3×10^{8}
393.4071	25 640.598	3	228.849	2	1.8×10^{8}
394.9825	29 766.188	5	4455.756	6	4.5×10^{8}*
395.6740	26 929.306	4	1663.120	3	8.5×10^{7}
395.6775	26 545.399	4	1279.424	4	1.1×10^{8}
395.7204	25 492.072	3	228.849	2	1.1×10^{8}
397.3998	26 545.399	4	1388.941	3	2.7×10^{8}
398.2165	27 313.506	6	2208.657	5	3.9×10^{8}
405.5836	25 928.289	5	1279.424	4	2.9×10^{8}
406.1800	28 812.043	6	4199.367	5	2.0×10^{8}
406.6914	28 557.829	7	3976.104	6	3.1×10^{8}
409.3287	26 632.010	5	2208.657	5	1.9×10^{8}
409.8139	28 812.043	6	4417.618	5	2.4×10^{8}
432.4595	23 117.060	5	0.000	4	1.1×10^{8}
434.3560	23 244.973	2	228.849	2	9.7×10^{7}
444.7667	22 477.386	3	0.000	4	5.0×10^{7}
450.1096	22 210.585	4	0.000	4	4.3×10^{7}
451.8019	22 127.392	3	0.000	4	5.5×10^{7}
452.1957	25 208.286	4	3100.151	4	1.2×10^{8}
453.1276	23 725.770	2	1663.120	3	8.9×10^{7}
453.1329	22 291.251	3	228.849	2	7.5×10^{7}
453.2009	23 722.196	4	1663.120	3	8.9×10^{7}
454.6061	22 219.750	2	228.849	2	6.3×10^{7}
455.2063	22 190.760	3	228.849	2	4.0×10^{7}
455.3064	23 620.200	2	1663.120	3	5.5×10^{7}
458.1098	25 134.962	3	3312.240	4	1.1×10^{8}
458.3089	21 813.247	3	0.000	4	3.7×10^{7}
461.0463	21 683.722	5	0.000	4	7.2×10^{7}
463.0779	23 251.722	4	1663.120	3	8.1×10^{7}
463.2322	21 581.408	5	0.000	4	1.7×10^{8}
464.0857	24 853.962	5	3312.240	4	1.8×10^{8}
464.1060	23 978.411	4	2437.629	4	1.5×10^{8}
464.9880	21 499.915	3	0.000	4	8.3×10^{7}
465.0509	21 725.865	1	228.849	2	1.2×10^{8}
467.0893	24 715.417	5	3312.240	4	1.4×10^{8}
467.4485	23 049.867	2	1663.120	3	1.4×10^{8}
469.0713	25 730.382	6	4417.618	5	1.6×10^{8}
469.6499	22 949.615	4	1663.120	3	1.1×10^{8}
470.6997	25 438.378	5	4199.367	5	1.5×10^{8}
472.4306	21 161.192	4	0.000	4	2.5×10^{7}
472.7562	21 375.475	2	228.849	2	2.7×10^{7}
473.3962	22 781.169	4	1663.120	3	6.7×10^{7}
473.4693	22 503.719	4	1388.941	3	7.0×10^{7}
474.4801	28 850.009	5	7780.202	6	3.3×10^{8}*
475.0829	23 251.722	4	2208.657	5	5.3×10^{7}

Table 1. (Continued.)

λ (nm)	E_u (cm^{-1})	J_u	E_l (cm^{-1})	J_l	$g_u A_{ul}$ (s^{-1})
475.2578	24 135.490	3	3100.151	4	6.5×10^7
476.4719	23 190.384	6	2208.657	5	5.2×10^7
477.5076	22 325.164	4	1388.941	3	4.3×10^7
477.5098	24 248.369	5	3312.240	4	5.3×10^7
478.6572	22 549.057	2	1663.120	3	6.4×10^7
478.8427	24 853.962	5	3976.104	6	1.6×10^8
480.8505	25 208.286	4	4417.618	5	1.2×10^8
482.0611	22 127.392	3	1388.941	3	5.0×10^7
482.2547	20 730.135	5	0.000	4	1.0×10^8
483.4052	23 049.867	2	2369.068	3	8.1×10^7
483.6706	21 948.875	3	1279.424	4	9.1×10^7
483.7475	23 978.411	4	3312.240	4	7.7×10^7
484.3055	22 851.015	6	2208.657	5	8.5×10^7
484.5534	20 631.804	5	0.000	4	8.6×10^7
484.7774	25 384.989	3	4762.718	4	3.6×10^8
485.3592	23 909.764	3	3312.240	4	9.9×10^7
486.1739	20 791.875	1	228.849	2	3.7×10^7
486.8651	21 813.247	3	1279.424	4	5.5×10^7
487.4354	20 509.805	4	0.000	4	4.1×10^7
488.1536	20 708.481	2	228.849	2	3.6×10^7
488.6175	29 839.334	3	9379.148	4	$2.3 \times 10^{8*}$
489.2851	20 661.129	3	228.849	2	3.0×10^7
489.8202	23 722.196	4	3312.240	4	8.7×10^7
490.8137	25 134.962	3	4766.323	2	7.9×10^7
491.9876	20 320.040	4	0.000	4	3.3×10^7
492.1925	25 058.207	6	4746.627	6	8.3×10^7
492.4251	21 581.408	5	1279.424	4	6.4×10^7
492.4896	26 538.263	6	6238.934	5	1.2×10^8
493.0537	20 276.120	5	0.000	4	1.8×10^7
493.0698	22 713.073	3	2437.629	4	3.8×10^7
493.9122	21 520.287	4	1279.424	4	7.4×10^7
494.0389	24 691.432	6	4455.756	6	6.9×10^7
494.8680	23 301.906	3	3100.151	4	5.0×10^7
494.8716	24 619.260	4	4417.618	5	4.5×10^7
495.1904	22 567.448	1	2378.827	2	2.4×10^7
495.1941	25 990.573	7	5802.108	7	6.1×10^7
495.4021	22 549.057	2	2369.068	3	4.2×10^7
495.5962	24 148.194	7	3976.104	6	6.1×10^7
496.6372	27 909.999	5	7780.202	6	2.0×10^8
497.1920	24 853.962	5	4746.627	6	9.6×10^7
497.4093	22 477.386	3	2378.827	2	5.6×10^7
498.7542	23 240.982	3	3196.607	4	1.3×10^8
498.8693	22 477.386	3	2437.629	4	6.6×10^7
500.4811	24 135.490	3	4160.283	3	7.1×10^7
500.9098	23 154.693	3	3196.607	4	3.0×10^8
501.2515	25 260.320	7	5315.803	7	1.3×10^8
501.3782	23 251.722	4	3312.240	4	5.8×10^7
501.6550	19 928.468	3	0.000	4	2.7×10^7
502.1443	23 885.162	5	3976.104	6	1.5×10^8
502.5152	24 660.675	2	4766.323	2	8.0×10^7
503.0641	23 083.233	5	3210.583	5	5.6×10^7
503.3854	28 463.492	5	8603.531	6	1.7×10^8
503.9733	21 499.915	3	1663.120	3	3.9×10^7
504.0846	23 596.416	4	3764.008	5	2.2×10^8
504.2084	23 139.791	3	3312.240	4	7.8×10^7
504.2236	25 346.707	2	5519.751	3	6.8×10^7
504.3198	29 202.304	4	9379.148	4	$2.3 \times 10^{8*}$
504.8830	22 170.124	2	2369.068	3	10.0×10^7
505.4182	21 059.520	5	1279.424	4	6.8×10^7
507.1550	21 375.475	2	1663.120	3	3.8×10^7
507.1775	27 491.670	6	7780.202	6	5.5×10^8
508.0469	21 340.864	3	1663.120	3	8.3×10^7
508.3549	24 412.448	5	4746.627	6	7.7×10^7
508.4465	26 836.434	4	7174.156	4	1.2×10^8
508.9620	26 498.929	3	6856.559	4	1.7×10^8
509.3372	23 391.896	4	3764.008	5	8.3×10^7
509.7261	22 713.073	3	3100.151	4	5.2×10^7
509.9375	21 267.903	4	1663.120	3	3.7×10^7
511.2703	24 009.430	5	4455.756	6	2.6×10^8
511.8883	22 740.645	5	3210.583	5	8.7×10^7
511.9510	25 431.677	1	5904.006	2	9.8×10^7
512.5009	23 962.481	5	4455.756	6	1.5×10^8
512.7930	27 551.129	6	8055.526	6	6.5×10^7
512.8021	26 843.555	3	7348.299	4	9.8×10^7
513.7780	25 260.320	7	5802.108	7	9.4×10^7
513.9766	20 730.135	5	1279.424	4	2.9×10^7
515.3907	25 734.430	3	6337.061	3	1.2×10^8
515.3987	23 596.416	4	4199.367	5	8.8×10^7
516.1484	27 149.080	7	7780.202	6	9.8×10^8
516.4375	27 593.641	3	8235.605	2	4.0×10^8
516.9233	23 513.352	4	4173.494	4	5.5×10^7
517.7729	22 518.695	5	3210.583	5	4.3×10^7
517.8676	23 722.196	4	4417.618	5	7.7×10^7
518.0884	19 296.353	4	0.000	4	5.8×10^7
518.1750	22 503.719	4	3210.583	5	5.0×10^7
518.9265	28 644.342	4	9379.148	4	2.9×10^8
519.1713	25 058.207	6	5802.108	7	2.0×10^8
520.0457	27 114.140	4	7890.429	4	9.5×10^7
520.2583	23 962.481	5	4746.627	6	1.2×10^8
520.4716	23 184.096	7	3976.104	6	8.1×10^7
520.8908	23 391.896	4	4199.367	5	7.2×10^7
521.1035	23 947.422	5	4762.718	4	9.7×10^7
521.1923	25 990.573	7	6809.128	8	5.6×10^8
521.6375	25 640.598	3	6475.540	4	1.4×10^8
522.1903	21 582.401	3	2437.629	4	6.8×10^7
522.3461	23 901.786	4	4762.718	4	4.4×10^8
522.6244	23 895.211	1	4766.323	2	6.0×10^7
522.9745	21 324.736	6	2208.657	5	1.8×10^8
523.0843	24 427.862	6	5315.803	7	1.5×10^8
523.3772	19 330.215	2	228.849	2	2.1×10^7
523.8474	22 184.376	5	3100.151	4	3.1×10^7
523.8902	21 520.287	4	2437.629	4	3.5×10^7
524.0123	23 251.722	4	4173.494	4	5.2×10^7
524.4502	21 499.915	3	2437.629	4	1.2×10^8
524.5276	20 338.893	5	1279.424	4	2.7×10^7
524.5916	23 819.871	5	4762.718	4	4.4×10^8
524.9160	20 708.481	2	1663.120	3	2.9×10^7
524.9606	22 355.991	5	3312.240	4	6.8×10^7
525.1056	26 972.051	6	7933.558	5	2.0×10^8
525.2021	24 041.686	3	5006.719	3	6.3×10^7
525.3414	21 399.014	3	2369.068	3	3.4×10^7
525.5980	28 353.870	6	9333.222	6	2.3×10^8
525.9921	21 375.475	2	2369.068	3	4.6×10^7
526.9514	21 340.864	3	2369.068	3	5.4×10^7
526.9545	23 978.411	4	5006.719	3	5.2×10^7
527.1808	22 063.708	4	3100.151	4	6.3×10^7
527.6244	27 551.129	6	8603.531	6	1.9×10^8
527.8430	29 613.602	5	10 673.847	6	$1.9 \times 10^{8*}$
528.1352	19 158.135	2	228.849	2	1.9×10^7
529.2447	23 049.867	2	4160.283	3	4.6×10^7
529.4953	23 627.278	6	4746.627	6	5.3×10^7
529.6563	22 851.015	6	3976.104	6	2.1×10^8
530.2113	24 657.245	8	5802.108	7	6.1×10^7
531.3926	25 987.414	5	7174.156	4	1.6×10^8
531.4843	22 970.284	2	4160.283	3	5.7×10^7
531.7592	21 237.916	3	2437.629	4	3.3×10^7
532.3283	26 713.745	4	7933.558	5	1.9×10^8
532.8082	22 739.355	7	3976.104	6	2.0×10^8

Table 1. (Continued.)

λ (nm)	E_u (cm^{-1})	J_u	E_l (cm^{-1})	J_l	$g_u A_{ul}$ (s^{-1})
533.2339	20 411.394	4	1663.120	3	3.7×10^7
533.4022	26 843.555	3	8101.187	2	1.1×10^8
533.4712	26 436.162	6	7696.210	6	1.0×10^8
534.0663	23 725.770	2	5006.719	3	5.0×10^7
534.0769	24 957.614	4	6238.934	5	3.7×10^7
534.5122	26 545.399	4	7841.955	5	1.1×10^8
534.9270	21 885.546	4	3196.607	4	3.2×10^7
535.0530	25 854.290	3	7169.751	3	1.6×10^8
535.0722	27 271.854	7	8587.973	7	1.1×10^8
535.1367	21 993.874	4	3312.240	4	4.0×10^7
535.2219	24 198.377	4	5519.751	3	5.0×10^7
535.5957	23 083.233	5	4417.618	5	4.3×10^7
535.9265	21 023.153	2	2369.068	3	3.2×10^7
535.9969	22 851.015	6	4199.367	5	6.5×10^7
536.2726	20 030.979	3	1388.941	3	1.4×10^7
536.7543	25 434.458	7	6809.128	8	1.0×10^8
536.9074	20 998.840	1	2378.827	2	3.7×10^7
537.0305	24 135.490	3	5519.751	3	7.6×10^7
537.1562	18 611.386	3	0.000	4	1.8×10^7
538.0114	22 781.169	4	4199.367	5	3.2×10^7
538.4118	22 741.485	4	4173.494	4	4.0×10^7
539.1822	24 445.454	2	5904.006	2	7.1×10^7
539.7638	20 730.135	5	2208.657	5	1.4×10^8
539.7993	25 987.414	5	7467.160	5	8.5×10^7
539.9057	23 727.513	3	5210.906	2	6.9×10^7
539.9555	25 863.180	4	7348.299	4	7.8×10^7
539.9597	21 725.348	5	3210.583	5	4.4×10^7
540.2559	24 024.353	2	5519.751	3	5.4×10^7
540.4357	25 668.215	4	7169.751	3	1.5×10^8
540.7668	21 683.722	5	3196.607	4	3.7×10^7
540.8365	24 960.288	4	6475.540	4	6.7×10^7
541.1538	24 712.835	6	6238.934	5	6.3×10^7
541.1764	21 683.722	5	3210.583	5	3.7×10^7
542.1291	25 297.222	3	6856.559	4	5.7×10^7
542.1376	30 738.142	5	12 297.781	5	$1.4 \times 10^{8*}$
542.2155	25 059.621	2	6621.892	3	3.4×10^7
542.2230	23 184.096	7	4746.627	6	2.2×10^7
542.2262	24 009.430	5	5572.074	4	4.3×10^7
542.6374	18 652.242	3	228.849	2	1.6×10^7
542.6602	21 619.232	4	3196.607	4	3.1×10^7
542.8264	27 796.140	5	9379.148	4	1.2×10^8
542.9422	20 791.875	1	2378.827	2	2.0×10^7
543.0530	23 620.200	2	5210.906	2	5.9×10^7
543.3343	21 499.915	3	3100.151	4	4.2×10^7
543.6040	24 294.652	2	5904.006	2	2.9×10^7
543.6107	23 962.481	5	5572.074	4	3.6×10^7
543.7862	24 619.260	4	6234.792	3	10.0×10^7
544.5434	18 587.749	2	228.849	2	2.1×10^7
544.6184	21 456.528	5	3100.151	4	4.1×10^7
546.0071	21 520.287	4	3210.583	5	7.0×10^7
546.0088	20 747.237	4	2437.629	4	1.7×10^7
547.2866	25 441.048	3	7174.156	4	1.2×10^8
547.3386	26 107.128	6	7841.955	5	1.4×10^8
547.7411	24 873.633	4	6621.892	3	6.6×10^7
548.1147	23 811.369	4	5572.074	4	6.2×10^7
548.1974	25 093.105	5	6856.559	4	1.9×10^8
548.3391	23 869.048	2	5637.233	1	4.2×10^7
548.3496	24 135.490	3	5904.006	2	6.2×10^7
549.1165	23 725.770	2	5519.751	3	8.2×10^7
550.6105	22 355.991	5	4199.367	5	2.5×10^7
550.6462	23 727.513	3	5572.074	4	4.6×10^7
551.0678	22 162.504	1	4020.954	1	5.7×10^7
551.4213	24 364.716	4	6234.792	3	7.1×10^7
551.7392	26 707.443	7	8587.973	7	1.2×10^8

Table 1. (Continued.)

λ (nm)	E_u (cm^{-1})	J_u	E_l (cm^{-1})	J_l	$g_u A_{ul}$ (s^{-1})
551.7844	24 352.787	3	6234.792	3	4.0×10^7
552.6075	23 301.906	3	5210.906	2	4.2×10^7
553.5230	21 161.192	4	3100.151	4	1.2×10^8
553.7535	21 153.703	5	3100.151	4	5.4×10^7
554.0541	26 351.090	4	8307.309	3	1.5×10^8
554.2714	23 673.890	1	5637.233	1	5.1×10^7
554.2866	26 545.399	4	8509.209	4	8.9×10^7
554.4621	22 190.760	3	4160.283	3	4.3×10^7
554.6511	23 596.416	4	5572.074	4	6.0×10^7
554.7500	24 325.115	1	6303.984	2	5.3×10^7
555.0658	22 184.376	5	4173.494	4	4.3×10^7
555.2269	18 005.652	3	0.000	4	9.3×10^6
555.8647	22 184.376	5	4199.367	5	3.2×10^7
555.9202	22 438.967	6	4455.756	6	1.0×10^8
556.0012	26 972.051	6	8991.451	5	5.5×10^7
556.2126	20 411.394	4	2437.629	4	1.2×10^7
556.3020	25 686.084	5	7715.236	5	1.9×10^8
556.4245	23 282.722	8	5315.803	7	8.9×10^7
556.4966	21 161.192	4	3196.607	4	1.8×10^8
556.5965	21 725.348	5	3764.008	5	1.7×10^8
556.6477	27 790.306	7	9830.608	6	1.6×10^8
556.9294	21 161.192	4	3210.583	5	2.6×10^7
557.2190	19 330.215	2	1388.941	3	2.2×10^7
557.5107	25 987.414	5	8055.526	6	4.9×10^7
557.7282	24 159.701	4	6234.792	3	6.9×10^7
558.2688	22 325.164	4	4417.618	5	4.5×10^7
558.4608	21 877.490	6	3976.104	6	3.4×10^7
558.6619	24 731.583	3	6836.628	2	3.7×10^7
558.8098	22 063.708	4	4173.494	4	3.2×10^7
558.9240	24 549.787	4	6663.226	5	4.3×10^7
559.0096	25 774.246	5	7890.429	4	5.7×10^7
559.0533	20 320.040	4	2437.629	4	2.1×10^7
559.3676	24 535.600	5	6663.226	5	6.3×10^7
559.3750	23 391.896	4	5519.751	3	4.3×10^7
560.1280	24 657.245	8	6809.128	8	5.3×10^8
560.6529	19 220.360	4	1388.941	3	2.2×10^7
561.6533	25 266.806	5	7467.160	5	5.1×10^7
562.0381	20 998.016	4	3210.583	5	3.0×10^7
562.3743	18 005.652	3	228.849	2	1.1×10^7
562.5245	22 518.695	5	4746.627	6	3.1×10^7
562.8210	24 619.260	4	6856.559	4	5.1×10^7
563.3037	21 946.849	5	4199.367	5	3.8×10^7
563.4444	19 406.157	3	1663.120	3	1.5×10^7
563.4516	24 364.716	4	6621.892	3	3.4×10^7
564.0100	21 885.546	4	4160.283	3	4.1×10^7
564.0791	22 933.990	1	5210.906	2	3.4×10^7
564.6585	21 725.865	1	4020.954	1	6.3×10^7
565.5140	21 877.490	6	4199.367	5	2.4×10^8
565.9793	18 943.013	5	1279.424	4	1.4×10^7
566.3198	21 813.247	3	4160.283	3	2.7×10^7
566.3462	20 030.979	3	2378.827	2	2.0×10^7
566.5407	22 063.708	4	4417.618	5	2.4×10^7
566.9959	20 842.504	6	3210.583	5	2.2×10^8
567.1423	24 290.594	5	6663.226	5	4.7×10^7
567.7219	22 355.991	5	4746.627	6	3.0×10^7
568.2765	18 871.606	4	1279.424	4	1.4×10^7
568.7818	23 811.369	4	6234.792	3	4.3×10^7
568.8491	22 321.098	6	4746.627	6	5.3×10^7
569.6993	22 864.055	8	5315.803	7	4.2×10^8
569.9226	24 350.503	9	6809.128	8	7.0×10^8
570.2388	20 631.804	5	3100.151	4	6.9×10^7
570.9058	23 083.233	5	5572.074	4	5.0×10^7
571.0035	24 364.716	4	6856.559	4	4.2×10^7
571.2287	21 661.537	3	4160.283	3	3.6×10^7

Table 1. (Continued.)

λ (nm)	E_u (cm^{-1})	J_u	E_l (cm^{-1})	J_l	$g_u A_{ul}$ (s^{-1})
571.9031	23 282.722	8	5802.108	7	3.9×10^8
571.9535	18 758.513	3	1279.424	4	1.1×10^7
572.6133	21 619.232	4	4160.283	3	3.6×10^7
572.9343	22 660.085	2	5210.906	2	2.8×10^7
572.9425	25 958.129	4	8509.209	4	5.0×10^7
573.5690	22 949.615	4	5519.751	3	5.3×10^7
574.4677	25 990.573	7	8587.973	7	1.1×10^8
574.6458	21 161.192	4	3764.008	5	2.3×10^7
574.8262	24 565.881	3	7174.156	4	4.4×10^7
574.8936	21 153.703	5	3764.008	5	3.2×10^7
575.2500	25 434.458	7	8055.526	6	6.3×10^7
575.8111	25 058.207	6	7696.210	6	1.4×10^8
576.0590	21 375.475	2	4020.954	1	2.1×10^7
576.4769	19 711.008	3	2369.068	3	2.9×10^7
576.9934	21 499.915	3	4173.494	4	4.4×10^7
577.4989	20 411.394	4	3100.151	4	3.0×10^7
578.2417	25 344.548	6	8055.526	6	1.5×10^8
578.2782	20 498.515	5	3210.583	5	2.3×10^7
578.6873	24 445.454	2	7169.751	3	5.0×10^7
578.7202	25 208.286	4	7933.558	5	6.8×10^7
579.1337	22 360.158	2	5097.777	1	3.1×10^7
579.4792	20 962.608	2	3710.513	1	1.9×10^7
579.6087	24 715.417	5	7467.160	5	1.3×10^8
581.1841	24 549.787	4	7348.299	4	5.2×10^7
581.2915	21 654.060	7	4455.756	6	1.6×10^8
581.5469	21 165.259	1	3974.503	0	2.4×10^7
582.0368	23 513.352	4	6337.061	3	1.2×10^8
583.4244	20 346.021	6	3210.583	5	3.0×10^7
584.3100	20 320.040	4	3210.583	5	1.9×10^7
584.6076	24 274.908	3	7174.156	4	5.9×10^7
584.8325	24 561.348	6	7467.160	5	1.3×10^8
585.1017	18 365.725	5	1279.424	4	2.5×10^7
585.1102	26 077.519	5	8991.451	5	1.3×10^8
585.3670	19 457.393	3	2378.827	2	3.8×10^7
585.7112	21 267.903	4	4199.367	5	7.1×10^7
585.8139	20 276.120	5	3210.583	5	3.4×10^7
587.3897	19 457.393	3	2437.629	4	1.8×10^7
587.8032	20 320.040	4	3312.240	4	2.0×10^7
588.8523	26 808.109	6	9830.608	6	1.3×10^8
589.2468	20 730.135	5	3764.008	5	2.4×10^7
589.7752	22 360.158	2	5409.236	2	3.2×10^7
589.9714	24 412.448	5	7467.160	5	5.1×10^7
590.1287	22 844.779	3	5904.006	2	6.2×10^7
590.7489	25 193.242	2	8270.249	3	6.1×10^7
590.9863	21 076.477	4	4160.283	3	8.0×10^7
591.0120	18 194.890	5	1279.424	4	4.1×10^7
592.4036	19 244.787	4	2369.068	3	2.7×10^7
592.8350	19 072.103	6	2208.657	5	7.0×10^7
593.2164	20 063.180	6	3210.583	5	3.3×10^7
593.8437	21 581.408	5	4746.627	6	4.0×10^7
594.0857	20 591.937	6	3764.008	5	2.1×10^8
594.7639	21 226.361	5	4417.618	5	4.3×10^7
595.1211	20 998.016	4	4199.367	5	2.3×10^7
596.3334	18 427.612	3	1663.120	3	1.3×10^7
596.4623	22 170.124	2	5409.236	2	2.4×10^7
596.6181	22 558.596	6	5802.108	7	6.8×10^7
597.2091	32 073.229	7	15 333.298	8	$6.2 \times 10^{8*}$
597.2787	21 948.875	3	5210.906	2	2.9×10^7
597.9370	17 998.974	4	1279.424	4	1.8×10^7
598.1196	30 286.465	7	13 572.014	7	$2.0 \times 10^{8*}$
600.0180	18 324.668	2	1663.120	3	1.3×10^7
600.7374	23 811.369	4	7169.751	3	6.8×10^7
601.6588	17 895.539	5	1279.424	4	2.0×10^7
602.7165	20 747.237	4	4160.283	3	2.8×10^7

Table 1. (Continued.)

λ (nm)	E_u (cm^{-1})	J_u	E_l (cm^{-1})	J_l	$g_u A_{ul}$ (s^{-1})
605.7505	17 892.814	4	1388.941	3	2.0×10^7
606.6747	18 141.848	4	1663.120	3	2.1×10^7
606.8638	23 282.722	8	6809.128	8	3.5×10^7
606.9484	24 167.499	6	7696.210	6	1.2×10^8
607.6606	24 148.194	7	7696.210	6	1.2×10^8
608.0369	28 555.941	5	12 114.115	4	1.9×10^8
608.1283	16 668.190	3	228.849	2	1.2×10^7
608.8955	28 229.328	4	11 810.672	4	1.9×10^8
609.3192	22 882.755	5	6475.540	4	8.9×10^7
609.9799	18 758.513	3	2369.068	3	1.4×10^7
611.1825	21 994.428	2	5637.233	1	2.6×10^7
611.1924	24 412.448	5	8055.526	6	3.7×10^7
611.8560	23 513.352	4	7174.156	4	5.4×10^7
611.8904	21 654.060	7	5315.803	7	3.9×10^7
611.9810	17 998.974	4	1663.120	3	1.0×10^7
612.4252	24 214.433	4	7890.429	4	4.3×10^7
613.0147	29 432.305	6	13 124.010	5	$1.5 \times 10^{8*}$
613.5453	24 009.430	5	7715.236	5	4.8×10^7
614.2923	20 730.135	5	4455.756	6	2.8×10^7
614.7842	22 063.473	7	5802.108	7	4.6×10^7
614.9562	21 023.153	2	4766.323	2	2.1×10^7
615.1719	20 411.394	4	4160.283	3	3.7×10^7
616.5452	28 922.881	3	12 707.976	2	$2.3 \times 10^{8*}$
618.6926	28 008.895	4	11 850.252	5	1.1×10^8
618.7973	16 384.741	3	228.849	2	1.0×10^7
619.5233	19 347.542	6	3210.583	5	2.1×10^7
619.5534	20 591.937	6	4455.756	6	3.3×10^7
619.8050	29 734.634	6	13 605.000	6	$2.8 \times 10^{8*}$
620.9555	19 296.353	4	3196.607	4	1.4×10^7
621.1046	20 842.504	6	4746.627	6	2.0×10^7
621.2288	24 148.194	7	8055.526	6	1.9×10^7
622.3255	17 343.734	5	1279.424	4	8.9×10^6
622.8233	16 051.478	4	0.000	4	6.6×10^6
624.1952	20 782.510	3	4766.323	2	8.6×10^6
625.3651	18 194.890	5	2208.657	5	1.6×10^7
625.6362	28 940.252	7	12 960.950	6	$1.3 \times 10^{8*}$
625.7991	29 099.164	5	13 124.010	5	$1.8 \times 10^{8*}$
626.4270	29 564.126	6	13 605.000	6	$2.3 \times 10^{8*}$
628.6387	23 370.168	6	7467.160	5	3.0×10^7
628.6430	30 511.959	7	14 609.088	7	$1.6 \times 10^{8*}$
630.6638	19 062.498	5	3210.583	5	1.8×10^7
631.7950	31 219.843	6	15 396.286	6	$1.5 \times 10^{8*}$
633.1973	16 017.358	3	228.849	2	6.1×10^6
635.3483	22 210.585	4	6475.540	4	2.1×10^7
638.6098	28 122.510	6	12 467.827	5	6.0×10^7
638.6257	21 226.361	5	5572.074	4	1.4×10^7
638.6845	27 766.972	4	12 114.115	4	2.4×10^8
639.0320	19 843.704	5	4199.367	5	1.4×10^7
639.9895	28 744.941	5	13 124.010	5	9.5×10^7
639.9941	22 477.386	3	6856.559	4	1.3×10^7
643.9966	17 892.814	4	2369.068	3	9.6×10^6
646.1881	19 235.098	6	3764.008	5	1.3×10^7
649.0973	22 064.966	6	6663.226	5	4.5×10^7
650.3980	19 347.064	5	3976.104	6	8.0×10^6
650.4125	19 544.105	4	4173.494	4	8.4×10^6
650.9009	15 587.927	2	228.849	2	5.1×10^6
651.7311	18 550.101	4	3210.583	5	2.2×10^7
653.0681	19 072.103	6	3764.008	5	1.0×10^7
656.0789	18 550.101	4	3312.240	4	9.1×10^6
657.3596	21 683.722	5	6475.540	4	2.6×10^7
657.7453	16 588.202	4	1388.941	3	5.1×10^6
659.9634	19 347.542	6	4199.367	5	1.2×10^7
660.5348	17 343.734	5	2208.657	5	7.8×10^6
662.2997	18 194.890	5	3100.151	4	1.3×10^7

Table 1. (Continued.)

λ (nm)	E_u (cm^{-1})	J_u	E_l (cm^{-1})	J_l	$g_u A_{ul}$ (s^{-1})
662.8931	17 289.878	6	2208.657	5	2.3×10^7
665.1430	20 346.021	6	5315.803	7	1.0×10^7
666.1412	22 355.991	5	7348.299	4	3.3×10^7
667.9795	18 942.478	7	3976.104	6	1.1×10^7
667.9875	18 987.150	2	4020.954	1	1.2×10^7
668.6599	27 912.105	6	12 960.950	6	1.6×10^8
671.0090	17 998.974	4	3100.151	4	4.9×10^6
671.3473	19 347.064	5	4455.756	6	1.3×10^7
672.6536	22 558.596	6	7696.210	6	1.4×10^7
674.9381	24 808.737	2	9996.647	3	3.0×10^7
674.9493	18 008.442	5	3196.607	4	9.3×10^6
676.4447	22 127.392	3	7348.299	4	2.2×10^7
676.7678	16 051.478	4	1279.424	4	5.3×10^6
677.0154	23 370.168	6	8603.531	6	2.1×10^7
677.8272	14 748.945	4	0.000	4	5.8×10^6
678.0712	18 943.013	5	4199.367	5	1.4×10^7
679.3841	27 909.999	5	13 194.849	4	8.3×10^7
680.1720	18 871.606	4	4173.494	4	8.9×10^6
680.7812	17 895.539	5	3210.583	5	1.9×10^7
680.8822	17 120.402	5	2437.629	4	1.0×10^7
681.1622	22 518.695	5	7841.955	5	2.4×10^7
681.5294	25 730.382	6	11 061.551	7	6.8×10^7
681.8226	16 051.478	4	1388.941	3	1.1×10^7
682.6441	19 062.498	5	4417.618	5	1.2×10^7
683.9973	24 934.358	2	10 318.438	3	2.5×10^7
684.4264	19 062.498	5	4455.756	6	7.9×10^6
684.7253	15 879.778	5	1279.424	4	9.2×10^6
685.3594	23 190.384	6	8603.531	6	3.8×10^7
688.5713	15 798.226	3	1279.424	4	2.2×10^6
689.3664	26 868.899	5	12 366.834	5	9.8×10^7
689.4558	16 869.253	4	2369.068	3	7.3×10^6
690.4577	22 321.098	6	7841.955	5	2.3×10^7
690.9352	22 184.376	5	7715.236	5	1.6×10^7
693.9446	14 635.243	1	228.849	2	5.7×10^6
699.9892	15 945.111	4	1663.120	3	7.2×10^6
699.9930	15 561.346	5	1279.424	4	6.6×10^6
701.3351	20 730.135	5	6475.540	4	1.6×10^7
701.4811	19 567.423	8	5315.803	7	1.2×10^7
701.7237	18 221.192	1	3974.503	0	1.0×10^7
701.8720	18 661.289	5	4417.618	5	7.4×10^6
701.8787	31 391.084	3	17 147.538	4	$1.4 \times 10^{8*}$
704.9733	18 201.970	1	4020.954	1	9.1×10^6
705.4510	26 538.263	6	12 366.834	5	1.1×10^8
706.0000	28 904.034	6	14 743.626	6	$1.7 \times 10^{8*}$
712.3445	20 509.805	4	6475.540	4	1.6×10^7
714.1425	17 975.060	6	3976.104	6	1.8×10^7
714.1694	15 277.852	3	1279.424	4	5.2×10^6
715.1668	16 347.978	2	2369.068	3	8.8×10^6
717.7444	20 591.937	6	6663.226	5	1.8×10^7
719.1715	16 338.704	4	2437.629	4	8.8×10^6
720.1886	13 881.444	5	0.000	4	7.2×10^6
720.3553	19 680.343	6	5802.108	7	1.9×10^7
721.0674	17 075.107	5	3210.583	5	1.2×10^7
721.3919	16 066.940	6	2208.657	5	5.6×10^6
721.7356	15 240.619	4	1388.941	3	1.1×10^7
724.1733	21 520.287	4	7715.236	5	3.4×10^7
726.2635	19 567.423	8	5802.108	7	2.2×10^7
727.9945	17 708.707	7	3976.104	6	8.3×10^6
732.9909	26 853.642	1	13 214.677	1	2.1×10^8
734.5620	17 770.105	2	4160.283	3	8.5×10^6
736.3090	15 240.619	4	1663.120	3	3.5×10^6
738.3738	23 370.168	6	9830.608	6	3.1×10^7
739.3405	18 284.583	5	4762.718	4	9.7×10^6
740.1267	15 945.111	4	2437.629	4	8.9×10^6
742.0997	16 668.190	3	3196.607	4	6.7×10^6
743.3083	17 649.036	6	4199.367	5	1.4×10^7
743.8557	17 895.539	5	4455.756	6	1.4×10^7
744.4436	15 798.226	3	2369.068	3	9.3×10^6
746.2316	15 766.048	3	2369.068	3	7.4×10^6
747.2412	28 122.510	6	14 743.626	6	1.4×10^8
747.8708	17 343.734	5	3976.104	6	7.9×10^6
750.0701	15 766.048	3	2437.629	4	7.4×10^6
750.9491	20 661.129	3	7348.299	4	2.3×10^7
753.3727	19 072.103	6	5802.108	7	1.7×10^7
753.9521	14 539.212	3	1279.424	4	3.0×10^6
755.1247	17 438.566	4	4199.367	5	1.2×10^7
756.2860	15 587.927	2	2369.068	3	7.8×10^6
756.3601	21 059.520	5	7841.955	5	2.8×10^7
760.3101	17 895.539	5	4746.627	6	1.3×10^7
763.2547	21 153.703	5	8055.526	6	2.2×10^7
764.6077	17 530.761	5	4455.756	6	1.4×10^7
764.7883	19 928.468	3	6856.559	4	2.2×10^7
773.2326	16 693.152	4	3764.008	5	1.0×10^7
774.3774	22 740.645	5	9830.608	6	2.1×10^7
776.2954	17 051.642	3	4173.494	4	6.6×10^6
776.9748	17 066.246	6	4199.367	5	7.7×10^6
779.7705	16 017.358	3	3196.607	4	8.9×10^6
780.6801	16 016.409	5	3210.583	5	4.4×10^6
781.2696	18 598.261	6	5802.108	7	1.2×10^7
783.5879	19 567.423	8	6809.128	8	1.9×10^7
786.4491	18 027.669	7	5315.803	7	1.6×10^7
787.4130	23 370.168	6	10 673.847	6	1.5×10^7
787.4224	20 411.394	4	7715.236	5	7.3×10^6
791.3517	19 296.353	4	6663.226	5	2.1×10^7
792.7719	17 066.246	6	4455.756	6	1.2×10^7
803.1447	16 903.380	5	4455.756	6	6.6×10^6
804.0018	15 644.943	6	3210.583	5	5.7×10^6
806.6908	17 708.707	7	5315.803	7	8.0×10^6
807.0714	16 586.423	5	4199.367	5	1.5×10^7
807.9373	17 120.402	5	4746.627	6	7.0×10^6
812.0360	14 748.945	4	2437.629	4	9.9×10^6
819.9291	18 427.612	3	6234.792	3	9.7×10^6
822.0701	15 371.647	4	3210.583	5	7.4×10^6
822.3609	16 903.380	5	4746.627	6	8.8×10^6
824.5195	13 513.875	4	1388.941	3	4.0×10^6
824.6820	23 184.096	7	11 061.551	7	2.9×10^7
826.1096	14 539.212	3	2437.629	4	7.7×10^6
830.0726	17 615.893	4	5572.074	4	4.0×10^6
831.0228	15 240.619	4	3210.583	5	7.3×10^6
831.2339	16 200.493	3	4173.494	4	7.5×10^6
839.6388	17 708.707	7	5802.108	7	1.3×10^7
849.5816	14 136.322	3	2369.068	3	6.7×10^6
856.7477	15 644.943	6	3976.104	6	6.8×10^6
861.2642	15 371.647	4	3764.008	5	8.5×10^6
878.2171	16 699.384	6	5315.803	7	1.1×10^7
881.0841	13 784.151	5	2437.629	4	6.9×10^6

Extending the validity of the derived parameters significantly outside this range should be done with caution because our analysis is entirely empirical and does not make any statement about actual conditions in the arc.

An estimate for the uncertainty in the 536 new transition probability values for lines originating from upper levels between 13 514 and 28 850 cm^{-1} is the root-mean-square deviation of the independently known gA values of Bisson

[2] from the gA values calculated with equation (3) using $T = 6200$ K and $\beta = 0.021$ nm s. This relative standard deviation is 0.30. We might then reasonably attribute a random uncertainty in the gA values for transitions originating in this energy range of ±35%. Of course, we can say nothing about possible systematic uncertainties. There are 23 lines in table 1 whose upper levels lie above 28 850 cm^{-1}, with none of these higher than 32 073 cm^{-1}. For these lines, we arbitrarily estimate the random uncertainty in the transition probabilities to be ±50%.

7. Summary

We have presented absolute radiative transition probabilities for 559 strong spectral lines of neutral cerium ranging in wavelength from 343.8 to 881.1 nm. Transition probability data have not previously been available for these lines. The upper levels for these transitions range from 13 514 to 32 073 cm^{-1}. The random uncertainty in the transition probabilities is ±35% for almost all lines.

Acknowledgments

The author thanks Bill Martin, Joe Reader and Wolfgang Wiese for the advice, guidance and data that have made this work possible.

References

[1] Meggers W F, Corliss C H and Scribner B F 1975 *Tables of Spectral Line Intensities (National Bureau of Standards Monograph* 145) (Washington, DC: US Government Printing Office)
[2] Bisson S E, Worden E F, Conway J G, Comaskey B, Stockdale J A D and Nehring F 1991 *J. Opt. Soc. Am.* B **8** 1545
[3] Martin W C, Zalubas R and Hagan L 1978 *Atomic Energy Levels—The Rare-Earth Elements (National Standard Reference Data System—National Bureau of Standards* 60) (Washington, DC: US Government Printing Office)
[4] Martin W C 1963 *J. Opt. Soc. Am.* **53** 1047
[5] Martin W C 1971 *Phys. Rev.* A **3** 1810
[6] Meggers W F, Corliss C H and Scribner B F 1961 *Tables of Spectral Line Intensities (National Bureau of Standards Monograph* 32) (Washington, DC: US Government Printing Office)
[7] Bisson S E, Comaskey B and Worden E F 1995 *J. Opt. Soc. Am.* B **12** 193
[8] Verges J, Corliss C H and Martin W C 1972 *J. Res. Natl. Bur. Stand.* A **76** 285
[9] Xu H L, Persson A and Svanberg S 2003 *Eur. Phys. J.* D **23** 233
[10] Li Z S, Lundberg H, Wahlgren G M and Sikström C M 2000 *Phys. Rev.* A **62** 032505
[11] Hartog E A D, Wickliffe M E and Lawler J E 1998 *J. Korean Phys. Soc.* **33** 214
[12] Cowley C R 1983 *Mon. Not. R. Astron. Soc.* **202** 14
[13] Allen C W and Assad A S 1957 *Mon. Not. R. Astron. Soc.* **117** 36
[14] Allen C W 1957 *Mon. Not. R. Astron. Soc.* **117** 622
[15] Corliss C H and Bozman W R 1962 *Experimental Transition Probabilities for Spectral Lines of Seventy Elements (National Bureau of Standards Monograph* 53) (Washington, DC: US Government Printing Office)
[16] Bridges J M and Wiese W L 1970 *Astro Phys. J.* **161** L71
[17] Cowley C R and Corliss C H 1983 *Mon. Not. R. Astron. Soc.* **203** 651
[18] Haverlag M 2005 *Phys. Scr.* T **119** 67